

Hydrogen Atom and Hydride Transfer in the Reactions of Chromium(IV) and Chromium(V) Complexes with Rhodium Hydrides. Crystal Structure of a Superoxorhodium(III) Product

Andreja Bakac^{*,†} and Ilija A. Guzei[‡]

Ames Laboratory and Chemistry Department, Iowa State University, Ames, Iowa 50011

Received September 14, 1999

The aquachromyl ion, $\text{Cr}^{\text{IV}}_{\text{aq}}\text{O}^{2+}$, reacts with the hydrides $\text{L}(\text{H}_2\text{O})\text{RhH}^{2+}$ ($\text{L} = \text{L}^1 = [14]\text{aneN}_4$ and $\text{L}^2 = \text{meso-Me}_6\text{-}[14]\text{aneN}_4$) in aqueous solutions in the presence of molecular oxygen to yield $\text{Cr}_{\text{aq}}^{3+}$ and the superoxo complexes $\text{L}(\text{H}_2\text{O})\text{RhOO}^{2+}$. At 25 °C, the rate constants are $\sim 10^4 \text{ M}^{-1} \text{ s}^{-1}$ ($\text{L} = \text{L}^1$) and $1.12 \times 10^3 \text{ M}^{-1} \text{ s}^{-1}$ ($\text{L} = \text{L}^2$). Both reactions exhibit a moderate deuterium isotope effect, $k_{\text{RhH}}/k_{\text{RhD}} = \sim 3$ (L^1) and 3.3 (L^2), but no solvent isotope effect, $k_{\text{H}_2\text{O}}/k_{\text{D}_2\text{O}} = 1$. The proposed mechanism involves hydrogen atom abstraction followed by the capture of $\text{LRh}(\text{H}_2\text{O})^{2+}$ with molecular oxygen. There is no evidence for the formation of $\text{L}(\text{H}_2\text{O})\text{Rh}^{2+}$ in the reaction between $\text{L}(\text{H}_2\text{O})\text{RhH}^{2+}$ and $(\text{salen})\text{Cr}^{\text{V}}\text{O}^+$. The proposed hydride transfer is supported by the magnitude of the rate constants ($\text{L} = \text{L}^1$, $k = 8800 \text{ M}^{-1} \text{ s}^{-1}$; $(\text{NH}_3)_4$, 2500; L^2 , 1000) and isotope effects ($\text{L} = \text{L}^1$, $k_{\text{ie}} = 5.4$; L^2 , 6.2). The superoxo complex $[\text{L}^1(\text{CH}_3\text{CN})\text{RhOO}](\text{CF}_3\text{SO}_3)_2 \cdot \text{H}_2\text{O}$ crystallizes with discrete anions, cations, and solvate water molecules in the lattice. All moieties are linked by a network of hydrogen bonds of nine different types. The complex crystallized in the triclinic space group $P\bar{1}$ with $a = 9.4257(5) \text{ \AA}$, $b = 13.4119(7) \text{ \AA}$, $c = 13.6140(7) \text{ \AA}$, $\alpha = 72.842(1)^\circ$, $\beta = 82.082(1)^\circ$, $\gamma = 75.414(1)^\circ$, $V = 1587.69(14) \text{ \AA}^3$, and $Z = 2$.

Introduction

The reduction of chromate to $\text{Cr}_{\text{aq}}^{3+}$ proceeds through one or both of the highly reactive intermediate oxidation states, $\text{Cr}^{\text{V}}_{\text{aq}}$ and $\text{Cr}^{\text{IV}}_{\text{aq}}$. Owing to the development of an alternative route to aquachromium(IV) ion,¹ the redox reactivity of this species toward several organic and inorganic materials has been explored,² despite the short lifetime of only $\sim 30 \text{ s}$ at room temperature in the absence of added reagents.¹ On the other hand, very little is known about $\text{Cr}^{\text{V}}_{\text{aq}}$, mainly because it disproportionates rapidly to $\text{Cr}(\text{VI})$ and $\text{Cr}(\text{III})$.³ The situation is reversed in the presence of stabilizing ligands, such as macrocycles and complexing anions, where $\text{Cr}(\text{V})$ is more stable and has received more attention^{4–7} because of its possible role in the carcinogenicity of chromate.^{8–11} Still, the number of detailed mechanistic studies of the reactions of $\text{Cr}(\text{V})$ is limited.^{4–7,12,13}

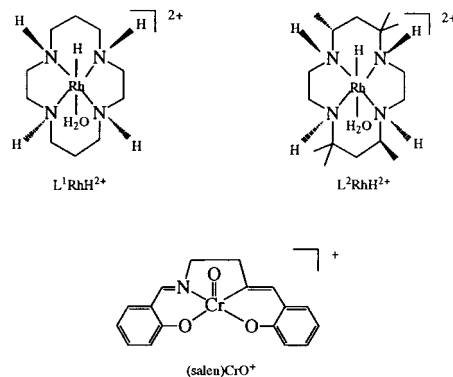
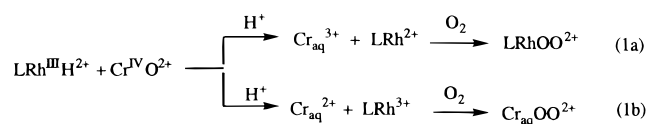


Figure 1. Structures of the macrocyclic rhodium hydrides and $\text{Cr}(\text{V})$ complex in this work.

This paper examines the redox reactivity of $\text{Cr}(\text{IV})$ and $\text{Cr}(\text{V})$ toward several substrates and addresses the preference for one-electron vs two-electron pathways for these two oxidation states in well-defined systems in aqueous solutions. The hydrides $(\text{NH}_3)_4(\text{H}_2\text{O})\text{RhH}^{2+}$, $([14]\text{aneN}_4)(\text{H}_2\text{O})\text{RhH}^{2+}$ (hereafter $\text{L}^1\text{-}(\text{H}_2\text{O})\text{RhH}^{2+}$), and $\text{meso-Me}_6\text{-}[14]\text{aneN}_4(\text{H}_2\text{O})\text{RhH}^{2+}$ (hereafter $\text{L}^2\text{-}(\text{H}_2\text{O})\text{RhH}^{2+}$), Figure 1, were chosen as substrates. An obvious advantage of the rhodium hydrides over many other compounds containing reactive element–hydrogen bonds is the ease with which one-electron and two-electron pathways can be identified. In the reaction between $\text{Cr}_{\text{aq}}^{2+}$ and $\text{L}(\text{H}_2\text{O})\text{RhH}^{2+}$ as an example, hydrogen atom transfer (one-electron path) produces $\text{LRh}(\text{H}_2\text{O})^{2+}$ and $\text{Cr}_{\text{aq}}^{3+}$, eq 1a. The hydride transfer (two-electron path) yields $\text{LRh}(\text{H}_2\text{O})_2^{3+}$ and $\text{Cr}_{\text{aq}}^{2+}$, eq 1b. If



[†] Ames Laboratory.

[‡] Chemistry Department.

- (1) Scott, S. L.; Bakac, A.; Espenson, J. H. *J. Am. Chem. Soc.* **1991**, *113*, 7787–7788.
- (2) Bakac, A.; Espenson, J. H. *Acc. Chem. Res.* **1993**, *26*, 519–523.
- (3) Buxton, G. V.; Djouider, F. *J. Chem. Soc., Faraday Trans.* **1996**, *92*, 4173–4176.
- (4) Krumpolc, M.; Rocek, J. *Inorg. Chem.* **1985**, *24*, 617–621.
- (5) Srinivasan, V. S.; Gould, E. S. *Inorg. Chem.* **1981**, *20*, 3176–3179.
- (6) Gould, E. S. *Acc. Chem. Res.* **1986**, *19*, 66–72.
- (7) Srinivasan, K.; Kochi, J. K. *Inorg. Chem.* **1985**, *24*, 4671–4679.
- (8) Farrell, R. P.; Lay, P. A. *Comments Inorg. Chem.* **1992**, *13*, 133–175.
- (9) Rossi, S. C.; Gorman, N.; Wetterhahn, K. E. *Chem. Res. Toxicol.* **1988**, *1*, 101–107.
- (10) Pratviel, G.; Bernadou, J.; Meunier, B. *Angew. Chem., Int. Ed. Engl.* **1995**, *34*, 746–769.
- (11) Pratviel, G.; Bernadou, J.; Meunier, B. *Adv. Inorg. Chem.* **1998**, *45*, 251–312.
- (12) Bakac, A. *Prog. Inorg. Chem.* **1995**, *43*, 267–351.
- (13) He, G.-X.; Arasasingham, R. D.; Zhang, G.-H.; Bruce, T. C. *J. Am. Chem. Soc.* **1991**, *113*, 9828–9833.

the reactions are carried out in the presence of O₂, the metal-(II) products L¹Rh(H₂O)²⁺ and/or Cr_{aq}²⁺ will be rapidly converted to their respective superoxo complexes, which can be identified unequivocally by their intense and distinct UV-vis spectra,^{12,14} eq 1 and Figure S-1.¹⁵ The formation of the superoxo products provides strong evidence for the intermediacy of the reduced metal ions, because all the known methods of generation of Cr_{aq}OO²⁺ and L(H₂O)RhOO²⁺ use the respective 2+ metal complexes as precursors.^{1,15}

Ideally, the chromium(IV) and chromium(V) complexes should have the same ligand system, leaving the oxidation state of the metal as the only variable in reactions with the rhodium hydrides. Unfortunately, this was not feasible in the present work because only certain combinations of the chromium oxidation states and chosen ligands are reasonably stable. The complexes used were Cr^{IV}_{aq}O²⁺ and (salen)Cr^VO⁺, Figure 1.

Experimental Section

Chloride salts of L(H₂O)RhH²⁺ and L(D₂O)RhD²⁺ (L = L¹, L²) and (NH₃)₄(H₂O)RhH²⁺ were prepared as previously described.^{14,16,17} The solid [L²(H₂O)RhH](CF₃SO₃)₂ was prepared by dissolution of the chloride salt in a minimum amount of water and precipitation with solid CF₃SO₃Li (Aldrich). The product was recrystallized twice from water. Chloride-free solutions of L¹(H₂O)RhH²⁺ in dilute perchloric or trifluoromethanesulfonic acid for kinetic purposes were prepared by ion exchange of the chloride salt.¹⁴ The compound [(salen)Cr(H₂O)₂]-Cl¹⁸ was converted to the triflate salt before the oxidation by PhIO to [(salen)CrO](CF₃SO₃)₂.⁷

For kinetic purposes the aquachromyl ion, Cr_{aq}O²⁺, was prepared¹ from Cr_{aq}²⁺ and limited amounts of O₂ in the presence of the desired rhodium hydride. The reactions were monitored at a maximum of the superoxorhodium products at 265 nm.

Kinetic and spectral measurements were carried out by use of a Shimadzu 3101 PC and Multispec 1500 spectrophotometers. An Applied Photophysics DX-17MV stopped-flow instrument was used to monitor the fast reactions of (salen)CrO⁺.

The solid superoxo complex [L²(CH₃CN)RhOO](CF₃SO₃)₂ for crystal structure determination was prepared as follows. A solution of 1 mM L²(H₂O)RhH²⁺ in 5 mM CF₃SO₃H (30 mL) was placed in a 10 cm quartz spectrophotometric cell, degassed with a stream of Ar, and photolyzed for 10 min in a Rayonet reactor to generate L²(H₂O)Rh²⁺. The solution was injected in 10 mL portions into 350 mL of O₂-saturated, ice-cold acetonitrile. The whole procedure was repeated one more time, and the combined acetonitrile solutions of L²(CH₃CN)-RhOO²⁺ were allowed to evaporate in a hood in the dark. Occasionally, the UV-vis spectrum of the solution was recorded. The position of the maximum absorbance in the visible changed from 430 nm (λ_{max} for L²(CH₃CN)RhOO²⁺) to ~470 nm (i.e., close to the 485 nm maximum for L²(H₂O)RhOO²⁺) as the solvent composition changed from mostly acetonitrile to mostly water. When the volume was reduced to ~15 mL, the solution was placed in a refrigerator. The needlelike orange crystals of [L²(CH₃CN)RhOO](CF₃SO₃)₂ appeared after several days.

Results

Reactions of Cr_{aq}O²⁺ with rhodium hydrides were carried out in the presence of O₂ to trap the reduced metal ion Cr_{aq}²⁺ or L(H₂O)Rh²⁺ (L = L¹ and L²) as a superoxo complex, eq 1. Figure S-2¹⁵ shows the spectrum of 0.10 mM L²(H₂O)RhH²⁺ before the reaction and the spectrum recorded immediately after the reaction with 0.012 mM Cr_{aq}O²⁺. The product spectrum is

Table 1. Summary of the Rate Constants (10³ M⁻¹ s⁻¹) for the Reactions of Oxochromium Complexes with Rhodium Hydrides in Aqueous Solution^a

	Cr ^{IV} _{aq} O ²⁺		(salen)Cr ^V O ⁺		Cr _{aq} OO ²⁺ ^b	
	k	k _H /k _D	k	k _H /k _D	k	k _H /k _D
L ¹ RhH ²⁺	~10		8.8		0.129	
L ¹ RhD ²⁺	2.7	~3	1.6	5.4	0.017	7.6
(NH ₃) ₄ RhH ²⁺			2.5		0.135	
L ² RhH ²⁺	1.12		1.0		0.024	
L ² RhD ²⁺	0.34	3.3	0.16	6.2		

^a [H⁺] = ionic strength = 0.10 M, 25 °C. Identical rate constants were obtained in H₂O and 90% D₂O/10% H₂O. ^b Reference 14a.

identical to that of L²(H₂O)RhOO²⁺ prepared independently from L²Rh(H₂O)²⁺ and O₂.¹⁴ The η¹ binding mode for O₂ in this superoxo complex has been confirmed by a crystal structure determination; see below. Similarly, the reaction of Cr_{aq}O²⁺ with L¹(H₂O)RhH²⁺ produced L¹Rh(H₂O)OO²⁺. The overall reaction between the rhodium hydrides and Cr_{aq}O²⁺ is therefore well represented by eq 1a.

The kinetics were determined in the presence of a large excess of rhodium hydride¹⁹ L¹(H₂O)RhH²⁺ (50 μM), L¹(H₂O)RhD²⁺ (30–150 μM), L²(H₂O)RhH²⁺ (30–200 μM), or L²(H₂O)RhD²⁺ (100–800 μM) over Cr_{aq}O²⁺ (5–50 μM) in 0.10 M HClO₄ at 25.0 ± 0.2 °C. Under these conditions the kinetics obeyed the rate law of eq 2, where k₀ represents the rate constant for the spontaneous decay of Cr_{aq}O²⁺, ~0.02 s⁻¹ at 25 °C.²⁰

$$-d[\text{Cr}_{\text{aq}}\text{O}^{2+}]/dt = (k_0 + k[\text{LRhH}^{2+}])[\text{Cr}_{\text{aq}}\text{O}^{2+}] \quad (2)$$

The reaction of L¹(H₂O)RhH²⁺ was too fast for a precise measurement, and the value listed in Table 1, ~10⁴ M⁻¹ s⁻¹, was estimated from the last 15–20% of the reaction.²¹ All the other values in Table 1, (2.70 ± 0.21) × 10³ M⁻¹ s⁻¹ (L¹(H₂O)-RhD²⁺), (1.12 ± 0.06) × 10³ (L²(H₂O)RhH²⁺), and (3.38 ± 0.11) × 10² (L²(H₂O)RhD²⁺), were obtained as slopes of the plots of k_{obs} against the average concentration of L(H₂O)-RhH²⁺,¹⁹ as shown in Figure 2. The values remained unchanged as the solvent H₂O was replaced by D₂O. Similarly, a decrease in [H⁺] from 0.10 to 0.040 M had no measurable kinetic effect. Concentrations of [H⁺] below 0.040 M were avoided to prevent the hydrolysis of various chromium species.

Reactions of (salen)CrO⁺ with Rhodium Hydrides. Submillimolar aqueous solutions of (salen)CrO⁺ were found to survive at room temperature for only 1–2 h. Detailed kinetics of the decay were not carried out, but the rate of absorbance decrease at the 600 nm maximum appeared to increase with time. On the basis of the UV-vis spectra, the decomposition product was identified as (salen)Cr(H₂O)₂⁺. The kinetic behavior of partly decomposed solutions of (salen)CrO⁺ was indistinguishable from that of freshly prepared solutions, once the decrease in concentration was taken into account. The spectrum in Figure S-3¹⁵ was run on a freshly prepared solution and the concentration calculated from the weight of the sample. The maximum in the visible range is more pronounced in water (λ_{max}

- (14) (a) Bakac, A. *J. Am. Chem. Soc.* **1997**, *119*, 10726–10731. (b) Bakac, A.; Thomas, L. M. *Inorg. Chem.* **1996**, *35*, 5880–5884.
 (15) Supporting Information.
 (16) Bakac, A. *Inorg. Chem.* **1998**, *37*, 3548–3552.
 (17) Thomas, K.; Osborn, J. A.; Powell, A. R.; Wilkinson, G. *J. Chem. Soc. A* **1968**, 1801–1806.
 (18) Yamada, S.; Iwasaki, K. *Bull. Chem. Soc. Jpn.* **1969**, *42*, 1463.

(19) The isotopic composition of the coordinated water, H₂O or D₂O, is the same as that of the solvent water.

(20) Scott, S. L.; Bakac, A.; Espenson, J. H. *J. Am. Chem. Soc.* **1992**, *114*, 4205–4213.

(21) The lifetime of Cr_{aq}O²⁺ (30 s) is too short for these experiments to be carried out in a stopped-flow instrument, because most of Cr_{aq}O²⁺ would decompose during the loading time. The other alternative, the generation of Cr_{aq}O²⁺ in situ, is not practical because it requires the handling of low concentrations of Cr_{aq}²⁺ (<0.4 mM) in the stopped-flow instrument.

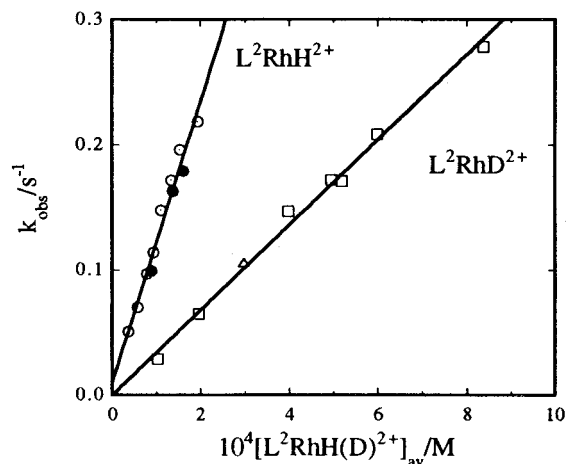


Figure 2. k_{obs} for $\text{L}^2(\text{H}_2\text{O})\text{RhH}^{2+}/\text{Cr}_{\text{aq}}\text{O}^{2+}$ reaction against the average concentration of $\text{L}^2(\text{H}_2\text{O})\text{RhH}^{2+}$ in H_2O (open circles) and D_2O (filled circles), and for $\text{L}^2(\text{D}_2\text{O})\text{RhD}^{2+}/\text{Cr}_{\text{aq}}\text{O}^{2+}$ reaction in 90% D_2O (squares). All the reactions had $[\text{H}^+] = 0.10 \text{ M}$, except for one run at 0.040 M H^+ (triangle).

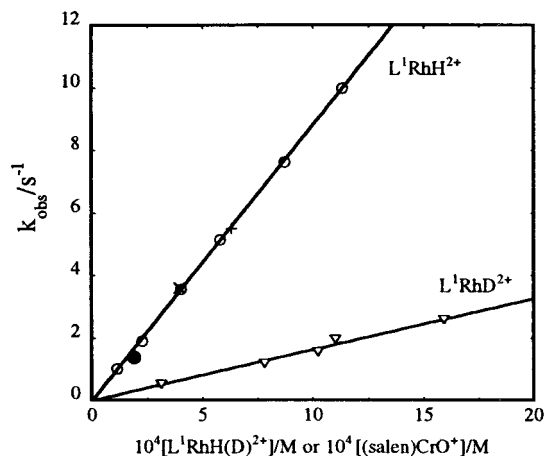
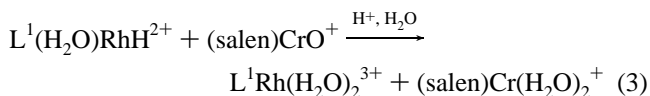


Figure 3. k_{obs} against the concentration of rhodium hydrides or $(\text{salen})\text{CrO}^+$ for the reaction between $(\text{salen})\text{CrO}^+$ and $\text{L}^1(\text{H}_2\text{O})\text{RhH}^{2+}$ in H_2O and $\text{L}^1(\text{D}_2\text{O})\text{RhD}^{2+}$ in 90% $\text{D}_2\text{O}/10\% \text{H}_2\text{O}$. Conditions: 25°C , ionic strength 0.10 M , $[\text{H}^+] = 0.10 \text{ M}$ (\circ and ∇), 0.010 M ($+$), and 7 mM (\times). One experiment (\bullet) used excess $(\text{salen})\text{CrO}^+$ and 0.3 mM H^+ .

$= 600 \text{ nm}$, $\epsilon = 2400 \text{ M}^{-1} \text{ cm}^{-1}$) than in acetonitrile ($\lambda \approx 550 \text{ nm}$ (sh), $\epsilon \approx 2000 \text{ M}^{-1} \text{ cm}^{-1}$).⁷

The reaction between $(\text{salen})\text{CrO}^+$ and $\text{L}^1(\text{H}_2\text{O})\text{RhH}^{2+}$ (eq 3) exhibits a 1:1 stoichiometry under both O_2 and Ar . The



kinetics and final spectra were also identical under the two sets of conditions, showing that free $\text{L}^1(\text{H}_2\text{O})\text{Rh}^{2+}$ was not produced in the reaction. Admittedly, the chromium product $(\text{salen})\text{Cr}(\text{H}_2\text{O})_2^+$ absorbs strongly at 265 nm ($\epsilon \approx 3 \times 10^4 \text{ M}^{-1} \text{ cm}^{-1}$), where $\text{L}^1(\text{H}_2\text{O})\text{RhOO}^{2+}$ exhibits a maximum ($\epsilon \approx 9 \times 10^3 \text{ M}^{-1} \text{ cm}^{-1}$), but even if only 20% of the reaction proceeded by a one-electron path, the $\text{L}^1(\text{H}_2\text{O})\text{RhOO}^{2+}$ would be detected. The Rh product is assumed to be $\text{L}^1\text{Rh}(\text{H}_2\text{O})_2^{3+}$, which has an intense, but featureless spectrum at $\lambda < 250 \text{ nm}$.

The reaction followed mixed second-order kinetics. The rate constant k_3 was determined from a plot of k_{obs} against the concentration of excess reagent, Figure 3. At a constant ionic strength of 0.1 M , the value is $8.8 \times 10^3 \text{ M}^{-1} \text{ s}^{-1}$, independent

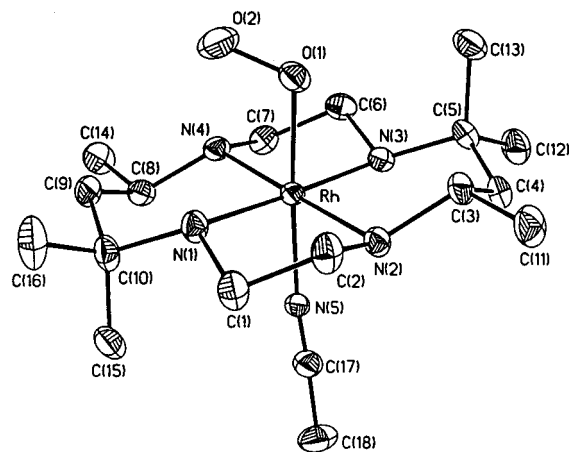


Figure 4. Perspective view of $\text{L}^2(\text{CH}_3\text{CN})\text{RhOO}^{2+}$ with the thermal ellipsoids at the 30% probability level. Selected bond distances (\AA) and angles ($^\circ$): $\text{Rh}-\text{O}(1) 2.005(3)$, $\text{Rh}-\text{N}(1) 2.076(4)$, $\text{Rh}-\text{N}(2) 2.067(4)$, $\text{Rh}-\text{N}(3) 2.100(4)$, $\text{Rh}-\text{N}(4) 2.062(4)$, $\text{Rh}-\text{N}(5) 2.045(4)$; $\text{O}(1)-\text{O}(2) 1.306(5)$, $\text{O}(1)-\text{Rh}-\text{N}(5) 177.15(13)$, $\text{O}(2)-\text{O}(1)-\text{Rh} 115.3(3)$.

of $[\text{H}^+]$ in the range $0.3-100 \text{ mM}$. The reaction exhibits a large kinetic isotope effect, $k_{\text{H}}/k_{\text{D}} = 5.4$. The tetraammine and L^2 complexes react somewhat more slowly, Table 1. The isotope effect for $\text{L}^2(\text{H}_2\text{O})\text{RhH}^{2+}$ is 6.2.

Crystal Structure of $\text{L}^2(\text{CH}_3\text{CN})\text{RhOO}^{2+}$. The molecular structure²² of the cation $\text{L}^2(\text{CH}_3\text{CN})\text{RhOO}^{2+}$ is shown in Figure 4. The Rh atom has a slightly distorted octahedral geometry with four nitrogen atoms in the equatorial plane and the acetonitrile and superoxo ligands in the apical positions. The Rh atom is coplanar with the four equatorial nitrogens to within 0.03 \AA , and the $\text{O}(1)-\text{Rh}-\text{N}(5)$ angle is $177.15(13)^\circ$. The average equatorial $\text{Rh}-\text{N}$ bond length is $2.076(16) \text{ \AA}$. The axial $\text{Rh}-\text{N}(5)$ bond distance, $2.045(4) \text{ \AA}$, is slightly shorter, but the difference is statistically insignificant. All the $\text{Rh}-\text{N}$ distances are in good agreement with the corresponding bonds in similar complexes and with the average $\text{Rh}-\text{N}$ single bond length of $2.063(56) \text{ \AA}$ obtained by averaging 1655 $\text{Rh}-\text{N}$ single bonds found in the Cambridge Structural Database (CSD).²³ The

- (22) X-ray crystal data for $\text{C}_{20}\text{H}_{41}\text{F}_6\text{N}_5\text{O}_9\text{RhS}_2$: triclinic, $P\bar{1}$, $a = 9.4257(5) \text{ \AA}$, $b = 13.4119(7) \text{ \AA}$, $c = 13.6140(7) \text{ \AA}$, $\alpha = 72.842(1)^\circ$, $\beta = 82.082(1)^\circ$, $\gamma = 75.414(1)^\circ$, $V = 1587.69(14) \text{ \AA}^3$, $Z = 2$, $T = 173(2) \text{ K}$, $D_{\text{calcd}} = 1.624 \text{ Mg/m}^3$, $R(F) = 5.49\%$ [$I > 2 \sigma(I)$]. The systematic absences in the diffraction data were consistent for the space groups $P1$ and $P\bar{1}$. The E-statistics strongly suggested the centrosymmetric space group $P\bar{1}$ that yielded chemically reasonable and computationally stable results of refinement. A successful solution by the direct methods provided most non-hydrogen atoms from the E-map. The remaining non-hydrogen atoms were located in an alternating series of least-squares cycles and difference Fourier maps. All non-hydrogen atoms were refined with anisotropic displacement coefficients except for several atoms in a triflate anion as described below. All hydrogen atoms were included in the structure factor calculation at idealized positions and were allowed to ride on the neighboring atoms with relative isotropic displacement coefficients. The absorption correction was based on fitting a function to the empirical transmission surface as sampled by multiple equivalent measurements (Blessing, R. H. *Acta Crystallogr.* **1995**, *A51*, 33–38). There is positional disorder present in both triflate anions. In one, atoms F(1), F(2), F(3), O(3), O(4), and O(5) are disordered over two positions each in a 70:30 ratio. These disordered atoms were refined isotropically. In the other molecule atoms F(4), F(5), and F(6) are equally disordered over two positions each. The triflate anions were refined with idealized geometries. There is also one solvate water molecule present in the asymmetric unit. The final difference Fourier map contained several small peaks (ca. $1.32-1.01 \text{ e/\AA}^3$) around the disordered atoms in the first triflate molecule and were considered noise. All software and sources of the scattering factors are contained in the SHELXTL (version 5.1) program library (G. Sheldrick, Bruker Analytical X-ray Systems, Madison, WI).
- (23) Allen, F. H.; Kennard, O. *Chem. Des. Automat. News* **1993**, *8*, 31–37.

Table 2. Likely Hydrogen-Bonding Interactions in [L²(CH₃CN)RhOO][CF₃SO₃]₂·H₂O

entry	donor	acceptor	distance, Å	angle, deg	type	strength
1	N(1)–H(1)	O(2), superoxo	2.847	126	intra, charge-assisted	weak
2	N(1)–H(1)	O(4), triflate	3.321	147	inter, charge-assisted	very weak
3	N(1)–H(1)	O(4'), triflate	3.197	132	inter, charge-assisted	weak
4	N(2)–H(2)	O(9), water	2.955	167	inter	medium
5	N(3)–H(3)	O(6), triflate	3.059	164	inter, charge-assisted	medium
6	N(4)–H(4)	O(2), superoxo	2.989	121.8	intra, charge-assisted	weak
7	N(4)–H(4)	O(2) [–x, 2 – y, –z], second superoxo	2.993	150.0	inter, charge-assisted	medium
8	O(9)–H(9C), water	O(5) [–x, 1 – y, –z], second triflate	2.889	149	inter, charge-assisted	medium
9	O(9)–H(9D), water	O(6) [–x, 1 – y, 1 – z], triflate	3.031	151	inter, charge-assisted	weak

Rh–O distance of 2.005(3) Å is somewhat shorter than the average Rh–O single bond of 2.055(35) Å as determined by averaging 1270 single Rh–O bonds in CSD.

The *R,R,S,S* stereochemistry around the nitrogens of the macrocyclic ligand is the same as that of the starting materials [L²RhCl₂]Cl²⁴ and [L²(H₂O)RhH](CF₃SO₃)₂,¹⁴ showing that no isomerization took place during the synthesis.

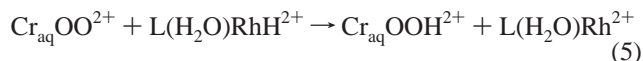
There are nine types of probable hydrogen-bonding interactions in the crystal structure of [L²(CH₃CN)RhOO][CF₃SO₃]₂·H₂O, Table 2. All the species in the lattice (the cation, two counterions, and water) form hydrogen bonds. The seven N–H···O bonds involve the N–H groups of the macrocycle, and the two O–H···O bonds are formed between the solvate water molecule and triflate anions (entries 8 and 9). Because of the ionic nature of the complex, all H bonds except one are considered charge assisted.²⁵ The assignment of bond strengths in Table 2 is based on bond distances and angles and the number of bonds to each H atom.²⁵ Two intramolecular hydrogen bonds are formed between the terminal oxygen of the coordinated superoxide and the N–H groups of the macrocycle, entries 1 and 6.

Discussion

Reactions with Cr_{aq}O²⁺. Earlier studies have demonstrated the ability of Cr_{aq}O²⁺ to react by one- and two-electron pathways. Most of the organic substrates examined in that work reacted by hydride transfer and yielded Cr_{aq}²⁺ and the two-electron-oxidized product, e.g., formaldehyde from methanol, eq 4. Hydrogen atom transfer was observed in exceptional cases, such as cyclobutanol and trimethylacetaldehyde, to yield the thermodynamically more favorable products.



In contrast to the organic substrates, the hydrides L(H₂O)RhH²⁺ prefer to react with Cr_{aq}O²⁺ in one-electron steps, eq 1a, as evidenced by the formation of superoxorhodium complexes in the presence of O₂. Another mechanism that could explain the formation of L(H₂O)RhOO²⁺ involves the initial generation of Cr_{aq}OO²⁺ in reaction 1b, followed by the known chemistry in eqs 5 and 6.¹⁴ This mechanism was dismissed on



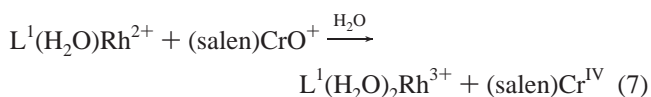
kinetic grounds. Reaction 1, which produces L(H₂O)RhOO²⁺ complexes with *k* = 10³–10⁴ M^{–1} s^{–1}, Table 1, is much faster

than hydrogen atom abstraction from rhodium hydrides by Cr_{aq}OO²⁺ in eq 5, *k*₅ ≤ 10² M^{–1} s^{–1},^{14a} which rules out reaction 5 as a step in the overall reaction.

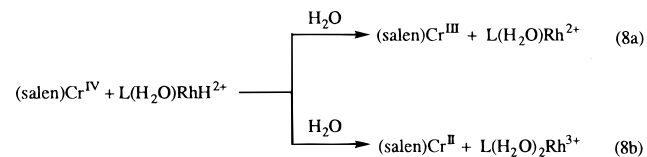
The kinetic deuterium isotope effect of about 3 (Table 1) for the two macrocyclic hydrides clearly shows that the breaking of the Rh–H bond is a part of the activation process. The observed hydrogen atom abstraction is fully consistent with the fact that the energy of the Rh–H bond in L(H₂O)RhH²⁺ is only ~250 kJ/mol,¹⁴ much less than the C–H bond energies²⁶ of the organic compounds that also react with Cr_{aq}O²⁺ by hydrogen atom transfer (cyclobutanol and pivalaldehyde).²⁰

The lack of solvent effect (H₂O vs D₂O) on the reaction rates is consistent with the extremely slow exchange of the rhodium-bound hydrogen with the solvent (*k* ≈ 10^{–6} s^{–1} for L = L¹).²⁷ It is somewhat surprising, although not unprecedented, that the replacement of H₂O by D₂O in the coordination sphere of Cr_{aq}O²⁺ has no effect on the kinetics. A similar behavior was observed in the reactions of Cr_{aq}OO²⁺ with the rhodium hydrides.¹⁴

Reactions with (salen)CrO²⁺. Several observations suggest that the reaction takes place by hydride transfer. First, oxygen-containing solutions do not produce L(H₂O)RhOO²⁺, making the involvement of LRh(H₂O)²⁺ highly unlikely. The reaction of LRh(H₂O)²⁺ with O₂ has a rate constant of 2.1 × 10⁸ M^{–1} s^{–1} (L = L¹) and 8.2 × 10⁷ (L²).¹⁴ If LRh(H₂O)²⁺ were produced, the rate constant *k*₇ would have to be close to 10¹⁰ M^{–1} s^{–1} for (salen)CrO⁺ to compete successfully for LRh(H₂O)²⁺, and even then there are conditions (1 mM O₂, 10 μM (salen)CrO⁺) that would lead to the formation of significant amounts of L(H₂O)RhOO²⁺. The complete lack of evidence for L(H₂O)RhOO²⁺ makes the mechanism of reactions 7 and 1b



quite unlikely. In addition, if reaction 7 were to take place, then the product (salen)Cr^{IV} would undoubtedly react with rhodium hydrides to produce either (salen)Cr²⁺ or LRh(H₂O)²⁺, eq 8,



just as Cr_{aq}O²⁺ does. Such a step would set up another competition between O₂ and (salen)CrO⁺ for the reductant produced, and possibly initiate a chain reaction (eqs 7 and 8a) if path 8a were to win over path 8b. The finding that the reaction

(24) Curtis, N. F.; Cook, D. F. *J. Chem. Soc., Dalton Trans.* **1972**, 691–697.

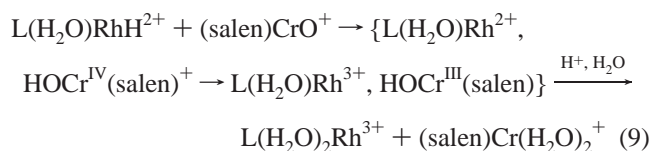
(25) Giacobozzo, C.; Monaco, H. L.; Viterbo, D.; Scordari, F.; Gilli, G.; Zanotti, G.; Catti, M. *Fundamentals of Crystallography*; Oxford University Press: Oxford, 1995.

(26) McMillen, D. F.; Golden, D. M. *Annu. Rev. Phys. Chem.* **1982**, *33*, 493–532.

(27) Unpublished observations.

proceeds with identical rate constants under all the conditions employed (Ar or O₂ atmosphere, large excess of either L(H₂O)-RhH²⁺ or (salen)CrO⁺) makes such a scheme highly improbable.

The Rh–H bond cleavage is obviously involved in the activation processes, as shown by large *k*'s of 5.4 (L = L¹) and 6.2 (L = L²). The hydrogen is believed to be transferred as hydride, although one cannot completely rule out a stepwise process involving Rh(II) and Cr(IV), followed by a rapid electron transfer within the solvent cage, as shown in eq 9. The



reaction inside the solvent cage should be fast in view of the large driving force (two reactive intermediates converted to two stable molecules), but the complete lack of dissociation of the initial products does seem unrealistic, especially because such a dissociation would be favored by electrostatic repulsion between the two cations.

The similarity between the rate constants for (salen)CrO⁺ and Cr_{aq}O²⁺ also argues against the same mechanism for the two reactions. The estimated reduction potential for Cr_{aq}O²⁺/Cr_{aq}³⁺ in aqueous solutions is >1.7 V vs NHE.¹² The one-electron reduction potential for (salen)CrO⁺/(salen)CrO in acetonitrile is 0.47 V against SCE.⁷ Even after the allowance is made for different solvents and different potential scales, the ion Cr_{aq}O²⁺ should still be a much more powerful one-electron reagent in aqueous solutions than (salen)CrO⁺. On the basis of the reduction potentials, the p*K*_a of Cr(H₂O)₆³⁺, and an estimated p*K*_a of <0 for (salen)Cr^{IV}OH⁺, the driving force for hydrogen atom abstraction from a common donor is ≥70 kJ/mol greater for Cr_{aq}O²⁺ than for (salen)Cr^VO⁺, making it highly improbable that the two oxidants react with such similar kinetics by the same mechanism. It seems purely coincidental that the rate constants for (salen)CrO⁺ and Cr_{aq}O²⁺ are nearly the same. This view is supported by the data for Cr_{aq}OO²⁺, a thermodynamically weaker one-electron oxidant and weaker H atom abstracting agent¹⁴ than Cr_{aq}O²⁺. As expected, Cr_{aq}OO²⁺ reacts by hydrogen atom abstraction more slowly than does Cr_{aq}O²⁺.

All the reactions in this work have sizable isotope effects, as expected for hydrogen atom and hydride transfer reactions. It is interesting to note, however, that hydrogen atom transfer to Cr_{aq}O²⁺ has a smaller *k* than the hydride transfer to (salen)-CrO⁺. One should expect the opposite order,²⁸ but the exceptions to this rule are too numerous²⁸ for any detailed mechanistic conclusions to be drawn from relative sizes of the *k*'s for the reactions studied.

(28) Stewart, R. *The Proton: Applications to Organic Chemistry*; Academic Press: Orlando, 1985; Chapter 4.

The crystal structure of L²(CH₃CN)RhOO²⁺ is the first such structure for a mononuclear superoxorhodium(III) complex. In support of the superoxo assignment, the O₂ unit is bound end-on, the Rh–O–O angle is 115.3 (3)°, and the O–O bond length is 1.306 (5) Å, well within the range of accepted bond distances for coordinated superoxide.^{12,29}

The terminal oxygen is directed toward the two nitrogens bearing the hydrogens on the “up” side of the equatorial plane. This geometry and the N–O distances of 2.85 and 2.99 Å, Table 2, suggest intramolecular hydrogen bonding between the terminal oxygen and the amine nitrogens. The bonding is, however, weak because it involves an unfavorable^{25,30} five-membered ring (Rh–O–O–H–N) and calculated NHO angles of only 126° and 122°. Consistent²⁵ with the weakness of the intramolecular bond, an intermolecular hydrogen bond to a triflate anion is also formed, entry 3 in Table 2. The results obtained here serve to strengthen our earlier conclusions, based on the resonance Raman data, about the involvement of hydrogen bonding in a related macrocyclic superoxochromium complex, L¹(H₂O)CrOO²⁺.³¹

Conclusions

In reactions with L(H₂O)RhH²⁺ complexes, there is a clear preference for hydrogen atom transfer by Cr^{IV}_{aq}O²⁺ (reaction 1) and for hydride transfer by (salen)Cr^VO⁺ (reaction 3). In neither case was there any evidence for the simultaneous operation of both pathways.

The detailed thermodynamic data for reactions 1a and 1b are not available, and it is not clear whether path 1a is favored on kinetic or thermodynamic grounds, but the stability of one set of products (Rh(II) + Cr(III)) is probably not very different from that of the other set (Rh(III) + Cr(II)).^{14b} In contrast, the chemistry of (salen)CrO⁺ is clearly determined by the thermodynamic preference for the two-electron path, as both metal complexes are produced in their most stable oxidation states.

Acknowledgment. This work was supported by the U.S. Department of Energy, Office of Basic Energy Sciences, Division of Chemical Sciences, under Contract W-7405-Eng-82. Useful discussions with Dr. J. H. Espenson are gratefully acknowledged.

Supporting Information Available: Figures showing UV–vis spectra of Cr_{aq}OO²⁺ and L²RhOO²⁺, the spectrum of L²RhH²⁺, the visible spectrum of (salen)CrO⁺, and two ORTEP drawings, X-ray crystallographic tables, and an X-ray crystallographic file, in CIF format. This material is available free of charge via the Internet at <http://pubs.acs.org>.

IC991098P

(29) Vaska, L. *Acc. Chem. Res.* **1976**, *9*, 175–183.

(30) Stout, G. H.; Jensen, L. H. *X-ray Structure Determination*; Wiley: New York, 1989; p 303.

(31) Bakac, A.; Scott, S. L.; Espenson, J. H.; Rodgers, K. L. *J. Am. Chem. Soc.* **1995**, *117*, 6483–6488.